

Structure and morphology of the Bosumtwi impact structure from seismic reflection data

Christopher A. SCHOLZ*, Tobias KARP, and Robert P. LYONS

Department of Earth Sciences, 204 Heroy Geology Laboratory, Syracuse University, Syracuse, New York 13244, USA

*Corresponding author. E-mail: cascholz@syr.edu

(Received 03 October 2006; revision accepted 21 December 2006)

Abstract—The Lake Bosumtwi impact structure in West Africa offers unparalleled opportunities for the study of cratering processes, as the structure is young (1.1 Myr) and minimally eroded. Because the center part of the structure is covered by Lake Bosumtwi, which is 8 km in diameter and ~70 m deep, it is possible to use marine-type seismic reflection techniques to obtain high-fidelity images of the lake subsurface, including key elements of the impact structure.

Eight profiles of multichannel seismic reflection (MCS) data were acquired in a radial pattern across the basin, as well as two other high-resolution seismic reflection surveys. The MCS data show a well-defined central uplift near the north-central part of the lake. Observed within the annular moat surrounding the buried central uplift is a section of post-impact lacustrine sediments more than 300 m thick. The central uplift structure has a diameter of 1.9 km and a maximum height of 130 m above the annular moat. The central uplift has an overall irregular upper surface with a small graben structure. We observe a series of normal faults that extend as much as 120 m into the sedimentary section above the central uplift. We interpret the normal faults to be a consequence of ongoing compaction of the high-porosity materials that comprise the central uplift. The interpreted impact structure surface, defined using seismic reflection data, was combined with regional topographic data from outside the lake in the form of a digital elevation model, which provides a useful perspective of overall impact structure morphology.

INTRODUCTION

Impact cratering was a critical process early in the Earth's history and has significantly affected the Earth's surface, atmosphere, and biosphere throughout geologic time (e.g., Grieve et al. 1995). Major craters on Earth complement analyses of craters of the other terrestrial planets, and studies of systematic changes in crater morphology with increasing size are characterized through a series of scaling laws (e.g., Croft 1985; Cintala and Grieve 1994). The ground-truth characterization of impact materials is possible primarily from the study of terrestrial impact craters and from examination of Apollo Moon mission samples.

Lake Bosumtwi in Ghana is perhaps the world's best-preserved complex crater, in large part because it formed relatively recently (1.07 Myr) (Koeberl et al. 1997) compared to most other large terrestrial craters. The crater rim measures 10.5 km in diameter, and the crater interior is covered by Lake Bosumtwi, which is ~8 km in diameter (Fig. 1). Because the regional bedrock of central Ghana is composed principally of 2 Gyr old metavolcanic and metasedimentary rocks of the

Birimian Supergroup (Jones et al. 1981; Leube et al. 1990), the resistant target rock rheologies may bear greater resemblance to the target materials of the other terrestrial planets than that of some other young craters observed on Earth.

Most of the interior of the Bosumtwi crater is covered by Lake Bosumtwi, which is one of the largest natural lakes in West Africa and is a site that has been intensively studied for its well-preserved, robust climate record of tropical West Africa (Talbot and Delibrias 1980). The closed-basin lake has a maximum water depth of ~75 m and is anoxic below a depth of ~15 m (Almond and Hecky, personal communication), although lake depth and also water column stratification vary significantly both seasonally and annually. In the early Holocene, the lake overflowed the crater rim and maintained a depth of ~150 m for several thousand years (Talbot and Delibrias 1980). Tropical lakes are known to accumulate organic-rich lacustrine sediments, and thus Lake Bosumtwi is commonly cited as a modern analogue for several ancient impact structures that contain economic reserves of oil and gas, such as the Ames and Red Wing Creek structures (e.g., Kirschner et al. 1991; Castañõ et al. 1997; Grieve 1997).

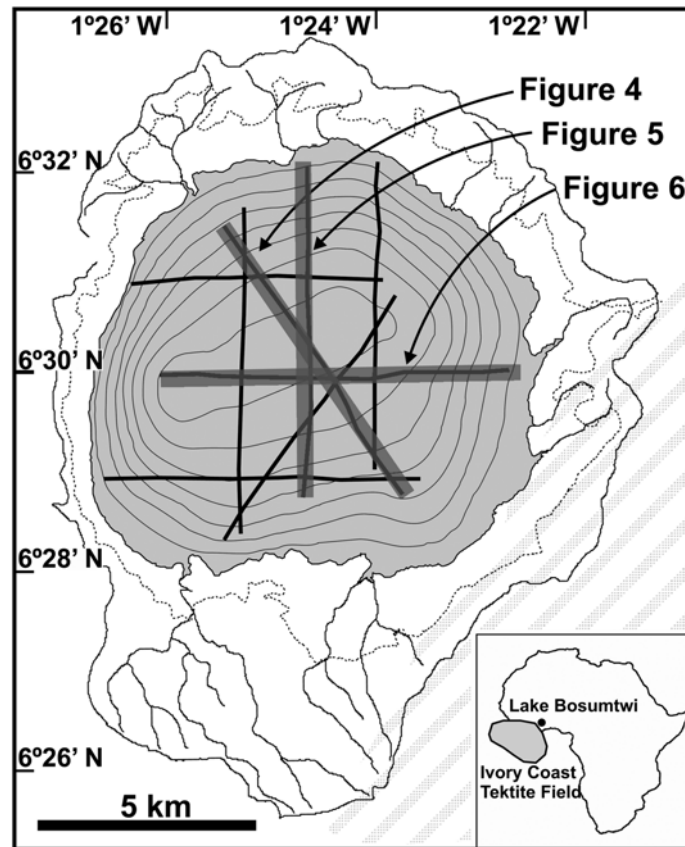


Fig. 1. Bathymetry and drainage area of Lake Bosumtwi, with multichannel seismic reflection profile locations. Shaded lines are presented in this paper. Dotted line = overflow level. Shaded region in the lower right (southeast) part of the area shows the location of the Obuom Range. Inset shows the location of the Bosumtwi impact structure in Africa, along with the location of the Ivory Coast tektite field.

In this study we used nested marine multichannel and single-channel seismic reflection data, augmented by wide-angle seismic records acquired using ocean-bottom hydrophones to assess the internal crater morphology, to determine the total thickness of post-impact lacustrine sediment in the crater, and to characterize the postulated central uplift. Results from several seismic reflection surveys are presented here, and were used to model the subsurface expression of the central part of the crater. This model was combined with a regional digital elevation model of the crater rim and outer ring to constrain the 2004 scientific drilling program on the lake and to help locate a transect of drillholes within the crater.

GEOLOGIC BACKGROUND AND PREVIOUS WORK

Central Ghana is underlain by the Proterozoic metavolcanic and metasedimentary rocks of the Birimian Supergroup (e.g., Leube et al. 1990; Attoh and Ekwueme 1997), which are the host rocks for the extensive Ghanaian gold deposits. The elevated Obuom Range borders the southeast part of the Lake Bosumtwi drainage basin (Fig. 1), and consists of uplifted metavolcanic rocks. Other than the

Obuom Range, the topography of the Lake Bosumtwi drainage basin follows the Pleistocene relief produced by the impact structure. Lake morphometry is that of a simple bowl-shaped depression, which developed from the accumulation of post-impact lacustrine and alluvial sediments (Fig. 1). The well-defined crater was initially characterized as a caldera (Smit 1964 and references therein) and has an average rim elevation of ~250 to ~300 m above the lake surface. At a radius of 8–10.5 km, an outer ring can be identified by low-relief topography (Wagner et al. 2002) and also by a halo-shaped magnetic anomaly observed in high-resolution aeromagnetic data (e.g., Plado et al. 2000). Initial suggestions of a meteorite impact origin for the Bosumtwi crater came from Maclaren (1931), and later publications by Smit (1964), Jones et al. (1981), Koeberl and Shirey (1993), and others present abundant evidence of a meteorite impact origin.

In addition to the reflection seismic studies undertaken on the lake and reported here, several other pre-drilling geophysical experiments were undertaken to characterize the basement structure. These include a seismic refraction experiment that used ocean-bottom hydrophones (Karp et al. 2000) as well as gravity and magnetic studies that were used

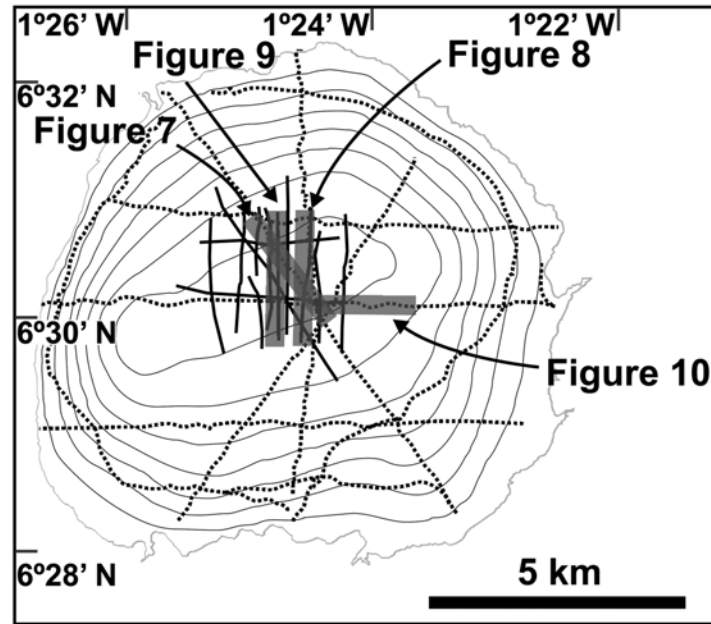


Fig. 2. Lake Bosumtwi bathymetry, showing positions of high-resolution CHIRP profiles (dotted lines) and 1 kHz "boomer" profiles (solid lines). Profiles presented in the paper are detailed subsets of the full-length profiles.

to corroborate the subsurface models. Initial results of the seismic reflection studies appear in Scholz et al. (2002) and Brooks et al. (2005). Recent aeromagnetic surveys (Plado et al. 2000) and Landsat TM data show that the ejecta blanket for the Bosumtwi structure extends 1–12 km from the center of the structure (Wagner et al. 2002).

METHODS

Three vintages of seismic reflection data were acquired on Lake Bosumtwi in 1999, 2000, and 2004, yielding differing resolution and maximum depths of subsurface penetration. All three surveys faced acquisition challenges unique to operating on this small, remote, tropical lake. These included difficulties of lake access, permitting from government and traditional authorities, and especially, extensive negotiations with the local fishing population. The latter issue proved challenging during all phases of geophysical data acquisition, as well as during the 2004 scientific drilling operation, because the artisanal fishery on Lake Bosumtwi uses fine-mesh set-nets for the harvesting of cichlid fishes for local consumption.

High-Resolution CHIRP Acquisition Program

During the 1999 field program, we used an Edgetech GEOSTAR "CHIRP" sub-bottom sonar system aboard a locally rented open boat to recover images of the uppermost part of the post-impact sediment column. This survey acquired 11 high-resolution single-channel seismic reflection profiles, totaling ~75 km in length, which were used to characterize the

shallow acoustic stratigraphy to a sub-bottom depth of ~50 m, plan the locations of the pre-drilling sediment piston cores, and identify reflection terminations indicative of water level variations (Fig. 2). The acquisition system uses a 4–24 kHz, Gaussian-shaped swept frequency signal, which yields a minimum resolvable bed thickness of 10 cm. During this survey, the acquisition system was interfaced with an autonomous global positioning system (GPS) navigation system. The acoustic source and hydrophone are embedded in a single tow fish, which was towed ~1 m off the side of a locally rented vessel, and ~1 m below the water surface. Seismic data were digitally recorded with a 0.02 ms sampling interval. Raw data files were processed using PROMAX processing software and the GPS navigation files were extracted from the SEG-Y formatted seismic files. The recovered data were of exceptionally high fidelity, and required no processing beyond the editing of header statics to adjust for time delays in acquisition, and for the removal of some zero-amplitude traces in limited areas. Edited lines were interpreted using Landmark Seisworks 2-D software, using standard seismic stratigraphic techniques (e.g., Vail 1987).

Multichannel Airgun Seismic Reflection Acquisition

Acquiring deep reflection images from below the post-impact sediments required using a long-offset receiving array, a larger active seismic source, and accordingly, involved bringing a significantly larger vessel to the lake. For this purpose, we used the R/V Kilindi, a modular catamaran owned and operated by Syracuse University for lake studies. The vessel consists of two fiberglass hulls connected with a

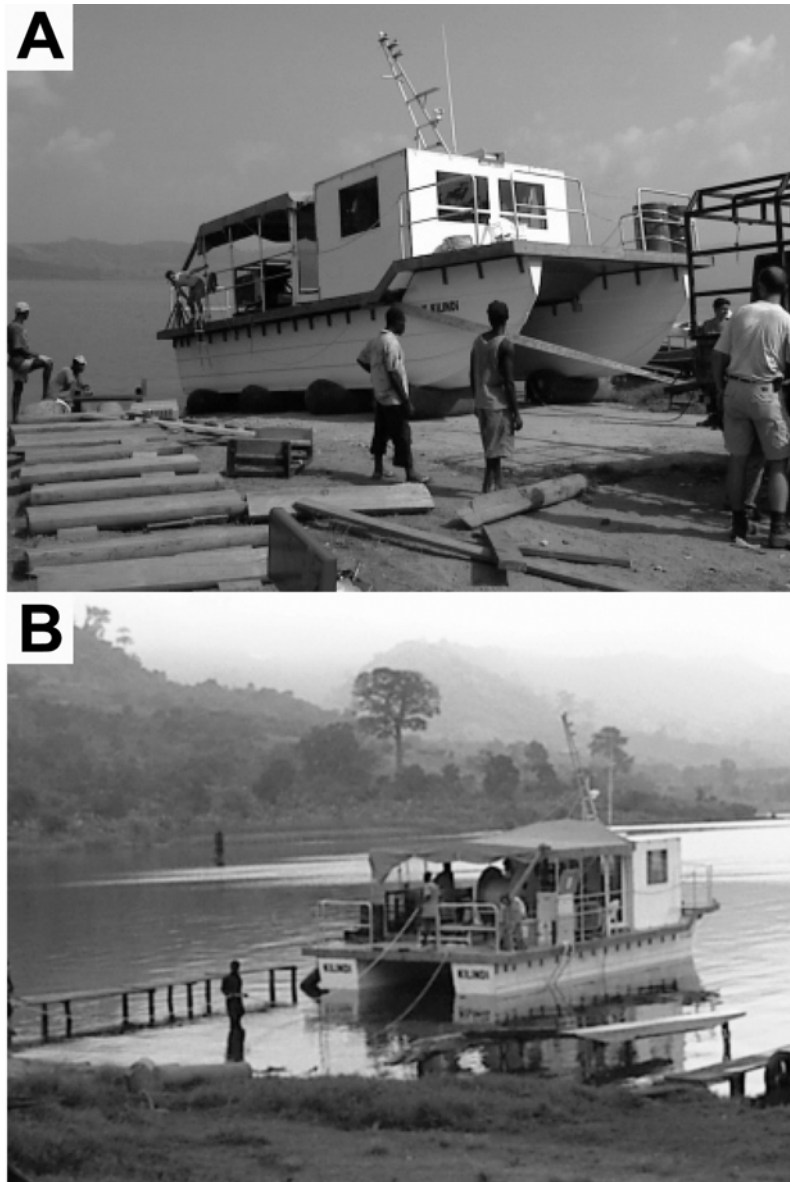


Fig. 3. Photos of the R/V Kilindi on Lake Bosumtwi. a) Launch of the catamaran research vessel across the lake shore using inflatable rubber rollers. The vessel was shipped to the lake in a shipping container and assembled by hand with the assistance of local residents. b) Loading the 600 m long hydrophone cable onto the vessel. This array was used during the multichannel seismic reflection survey, along with a mini GI gun as the seismic source.

steel framework, aluminum deck, and fiberglass laboratory-deckhouse. In 1999, it was shipped lakeside in a 40-foot shipping container and assembled by hand on the lakeshore using a small team of researchers assisted by 25 local laborers. To launch the 40 × 18-foot vessel we used a series of large, inflatable roller tubes which could easily support the weight of the vessel, and then rolled the vessel into the lake (Fig. 3).

For the seismic source we used a “mini-GI” airgun (35–35 cubic inches or 0.57–0.57 L), fired at 2000 PSI, which was powered by two diesel-driven high-pressure air compressors. The receiving array consisted of a 600 m, 48-

channel streamer (Fig. 1), and signals were acquired using an OYO DAS-1 system. We used a differential GPS system for navigation. Eight 24-fold profiles were acquired (Fig. 1), and data were processed using standard processing routines using Landmark PROMAX software through finite-difference time migration, and then depth converted. These data were complemented by data collected during a wide-angle refraction experiment (e.g., Karp et al. 2000), which used a 52-cubic-inch (0.85 L) airgun as the source, and three ocean-bottom hydrophones for receivers. Processed data were interpreted using Landmark Seisworks 2-D interactive interpretation and OPENVISION 3-D visualization software.

Because Lake Bosumtwi is considered a sacred lake by the local Ashanti people, metal objects are normally not permitted in the lake. However, the research team was granted permission to launch the R/V Kilindi and the geophysical equipment following a review and ceremonial dedication by the traditional authorities, including 25 local chiefs. Following data collection in 2000 and a subsequent shallow coring program, the R/V Kilindi was removed from the lake in 2001.

1 kHz “Boomer” Reflection Seismic Data Acquisition Program

In 2004, the R/V Kilindi was returned to Lake Bosumtwi to collect additional final site survey data and provide operational support for the 2004 Lake Bosumtwi scientific drilling project. Prior to the launch of the drilling barge, we planned to collect 3-D seismic data from the center part of the lake basin, based on initial results of the earlier seismic reflection studies (e.g., Scholz et al. 2002; Brooks et al. 2005). During the initial parameter testing effort, it became evident that the density of the fishing nets had increased since the previous field studies and that the collection of a true 3-D data volume could not be completed without removing the entire array of closely spaced fishing nets. Because this would have subjected the local fishing community to economic hardship during the period of net removal, we chose instead to complete a dense 2-D survey grid over the center part of the lake, in the vicinity of the planned drill sites (Fig. 2).

As the seismic source we used a Geoacoustics GEOPULSE “boomer” type source, selecting an output of 280 J. Incoming acoustic returns were collected using a Benthos single-channel hydrophone streamer, and recorded using TritonElics Delph2 seismic acquisition system. Navigational data were acquired using a differential GPS system. Fourteen boomer single-channel profiles were collected in the center of the lake, where obstructions from fishing nets were fewer in number than on the lake margins. Data processing of the boomer data was completed using Landmark PROMAX software and included trace editing, filtering, horizontal stacking of adjacent traces, and application of AGC (automatic gain control) using a 200 ms window. Data were interpreted along with the other vintages of reflection seismic data using Landmark Seisworks 2-D interpretation software.

Data Reduction, Interpretation, and Integration

Following the completion of data interpretation of the multichannel seismic data sets, the interpreted “basement” horizon was digitized using standard techniques. Fault interpretations were based on the fine-scale relief on sediment-impact rock interface, and upon the offset of reflections within the post-impact sedimentary section. Using

regional 15-minute topographic quadrangle maps published by the Ghana Department of Surveys, elevation above lake level was digitized at a 50-foot contour interval. This was merged with the depth-converted basement subsurface map derived from seismic reflection data generated using Landmark Seisworks software. The merged data were converted to a triangulated irregular network (TIN) using ARCGIS software. This TIN was then gridded at 4 m cell size spacing, exported as an ASCII text file, and regridded in Landmark Z-Map software at a 20 m cell interval. The final model was then imported into Openvision for 3-D visualization.

RESULTS AND INTERPRETATIONS

Multichannel Seismic Reflection Results

The airgun-sourced multichannel seismic reflection (MCS) data yield the most important results relevant to the morphology of the Bosumtwi impact structure. Significantly, none of the reflection data provide information below the contact between the post-impact sediments and the uppermost crater material. Additionally, considerable accumulation of biogenic gas in post-impact, organic-rich lacustrine sediments is evident on all vintages of data on the margins of the lake, which both obscures the near surface stratigraphy within sedimentary section in this area and induces numerous high-amplitude water bottom multiples on all profiles, from the lakeshore to within ~2 km of the basin center. Whereas the imaging effectively failed on the edges of the lake, data acquired from the central basin of the lake are of excellent quality and both the lacustrine stratigraphy and impact material surface are well imaged in that locality.

The most significant set of features revealed in the MCS data set define a distinctive central uplift situated just northwest of the center of the lake and crater (Fig. 4), and is observed on four radial images that criss-cross the center of the basin (Figs. 1, 4–6). The feature is 1.9 km in diameter, with a maximum height of ~130 m above the adjacent circular moat that surrounds the uplift and forms the deepest part of the crater floor. Above the crater floor, we observe as much as ~310 m of post-impact lacustrine sediment, but the peak of the central uplift is within ~150 m of the lake bottom at one location. The maximum crater rim-to-floor height is 750 m, measured from the maximum elevation of the crater rim to the base of the post-impact lacustrine sediments. The sedimentary section in the basin center is well characterized with the lacustrine section observed as a set of continuous reflections. The crater floor–post-impact sediment interface is easily identified on the MCS records as a moderate-low frequency, discontinuous, and high-amplitude package of irregular reflections, suggesting that the crater floor topography in the vicinity of the central uplift is broken and uneven (Figs. 4–6).

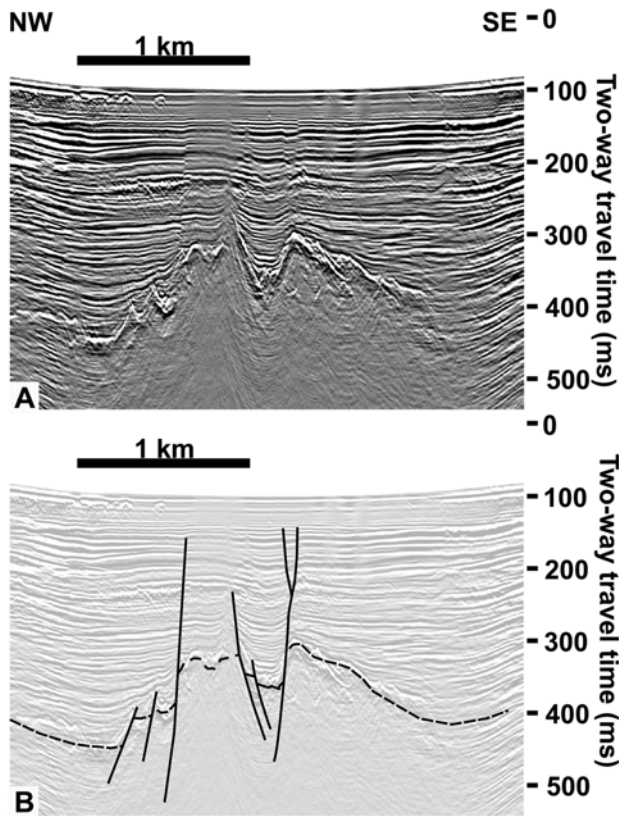


Fig. 4. a) Uninterpreted and (b) interpreted MCS profile 1 extending across the lake from northwest to southeast (central part of profile is shown). Note the pronounced central graben on the central uplift. The zone immediately beneath the central uplift is largely reflection-free, and is interpreted as mainly impact breccia. Several normal faults extend from the central uplift into the sediment section, and are interpreted as associated with post-impact compaction. The sediment-breccia interface is well imaged over most of the profile, and is characterized by a high-amplitude two-cycle reflection. Lower amplitude reflections observed beneath the sediment-breccia contact on the basin margins are mainly reverberations.

At the peak of the central uplift, we observe a distinctive graben that has a maximum depth of over 50 m (Fig. 4). Extending from the uplift surface into the sediment column we observe a series of faults that appear to have their origins on the graben boundary, and then extend upward 100 m or more into the sediment section that overlies the uplift. Other than the graben structure, the uplift is broadly symmetrical but with a broken second order relief indicative of fractured and deformed materials.

Boomer and CHIRP Data Set Results

The CHIRP and the 1 kHz boomer data sets were acquired mainly to help site paleoclimate drilling and coring sites in the post-impact sediments (Fig. 2) (e.g., Brooks et al. 2005; Peck et al. 2005), and neither data set provides images or direct information on the details of the central uplift or

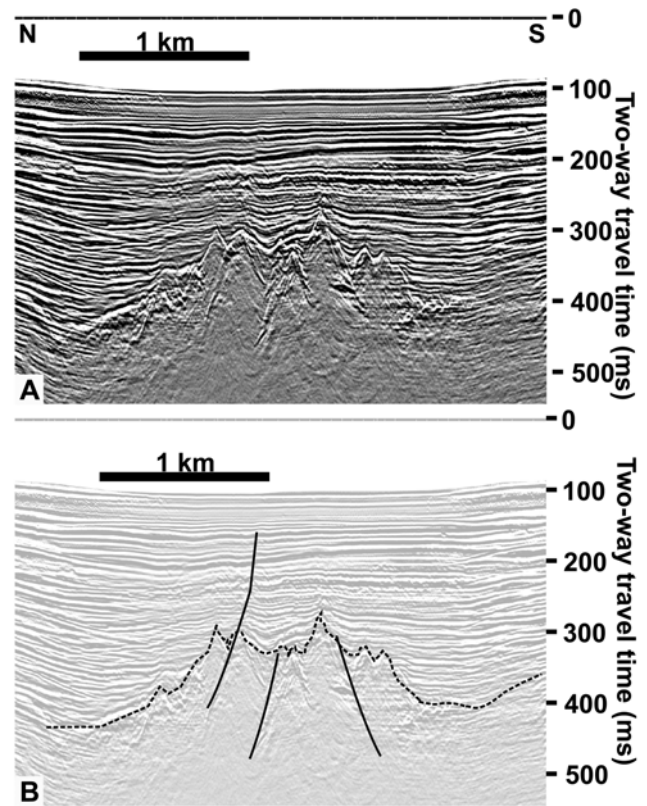


Fig. 5 a) Uninterpreted and (b) interpreted profile 4 extending across the central part of the lake from north to south. The central graben is not observed on this profile. Note several normal faults that extend up into the sediment section. The uppermost ~40 ms (TWTT) of sediment section contains distinctly lower amplitudes than the deeper sediment section reflections. This sequence is composed of high water content lacustrine muds, sitting on top of a desiccation surface. The edge of the annular moat is observed on the margins of this profile.

other aspects of the crater floor. However, both sets of data show evidence of offsets of the faults that extend upward into the sediment column from the top of the central uplift (Figs. 7–10). Because several intervals on either side of the normal faults show thickening of the sediment sequences from the footwall to the hanging wall (e.g., Fig. 7), this indicates episodic fault movement relatively recently in the history of the lake basin. Based on correlation of offset seismic reflections to dated intervals within the sediment drill cores recovered in 2004, it appears that the faults have been active within the past 150 kyr.

The deformation within the post-impact lacustrine section is clearly related to faults within the central uplift, and we interpret this deformation to be primarily due to differential compaction within the high-porosity pulverized impact rocks that comprise the bulk of the central uplift (Koeberl et al. 2007). Although these faults were active relatively recently, it is possible they formed during the collapse of the transient crater and were later reactivated.

The normal faults with the most offset in the sediment column are observed to extend from either the steep sides of the central uplift or from the central graben over the center of the uplift. These faults displace the lacustrine sediments approximately 1–3 m in the upper part of the sediment section; a maximum offset of 15 m is seen just above the central graben. Concentric faults are known to characterize many large complex craters (e.g., Chesapeake) (Poag et al. 1999), but none are clearly observed in these subsurface seismic reflection data. One possible exception is a deep offset on the crater floor observed in the southwest sector of the lake. We cannot rule out the possibility that concentric faults could exist on the margins of the basin in the area obscured by the gas. Subtle bathymetric terraces are observed in CHIRP and MCS data at water depths of ~60 m and ~72 m (Brooks et al. 2005), and are interpreted to be wave-cut terraces produced during prior low-lake stages (e.g., Talbot and Delibrias 1980). Alternatively, this subtle relief could indicate deep offsets in the crater material, associated with concentric normal faults. No radial faults were directly observed in the Lake Bosumtwi seismic reflection data.

As is typical of many modern lacustrine basins, seismic velocities are low throughout the sedimentary section, averaging less than 1600 m/s. Such low values are due to the high water content of near-surface sediments (e.g., Peck et al. 2005), which is as much as 90 wt%, producing saturated bulk-density values as low as 1.1 g/cm³ (Brooks et al. 2005). Abundant biogenic gas due to decay of the abundant organic materials in the near-surface sediments may also contribute to the observed low seismic velocity values. Velocities below the lake sediments are obtained from both MCS semblance analyses (interval velocities) and from wide-angle ocean-bottom hydrophone seismic records (Scholz et al. 2002; Karp et al. 2000), suggesting values of ~3200 m/s, compared with the Proterozoic regional bedrock velocities >5000 m/s (Karp et al. 2000).

DISCUSSION

The images acquired from the airgun-multichannel seismic reflection data were particularly useful for constraining the geometry of the central part of the Bosumtwi impact structure, and for siting the Bosumtwi drilling project drillholes into the impact rock material below the post-impact lacustrine sedimentary section. These data and also the high-resolution single channel data are proving valuable in deciphering the climate record stored in the lacustrine section (e.g., Peck et al. 2005; Brooks et al. 2005).

The radial framework of deep basin seismic reflection lines allows us to interpret a three-dimensional surface representing the contact between the post-impact sediments and extending around the entire central part of the impact structure (Fig. 11). This interpreted surface was combined

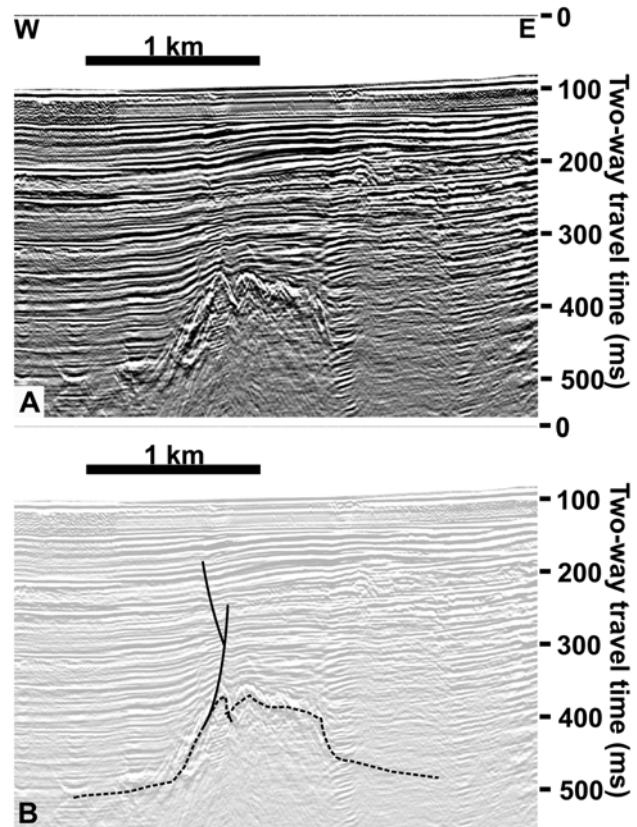


Fig. 6. a) Uninterpreted and (b) interpreted MCS profile 3 extending across the central part of the lake from west to east. Observed on the west side of this profile is the thickest part of the Lake Bosumtwi sediment section. The central uplift displays an apparent asymmetry on this profile, with an extremely steep western flank. Note the normal fault that extends from this escarpment up into the sediment section, perhaps implying differential compaction-related subsidence along this line of section.

with regional topographic data, originally scanned and digitized from topographic quadrangle maps, then regridded to form a combined impact structure surface (Fig. 11). The resulting digital elevation model presents the well-defined main rim structure, an outer ring with a mean elevation of <30 m above the surrounding terrain, and the central uplift. The central uplift is roughly circular around its base and displays a rugged topography, including a central graben structure that is ~15 m deep. Whereas the existing data are insufficient to completely resolve the geometry of the central graben structure, it appears to be approximately symmetrical, and to extend in an east-west orientation across the uplift.

The uplift is situated slightly off-center of the main crater, ~1 km to the north of the geometric center of the crater. This mild asymmetry may be a useful constraint in assessing the trajectory angle of the Bosumtwi impactor. Assessing the angle of impact requires analyses of the geometry and degree of symmetry of the interior structure or uplift, and asymmetries in the ejecta blanket or crater rim deformation

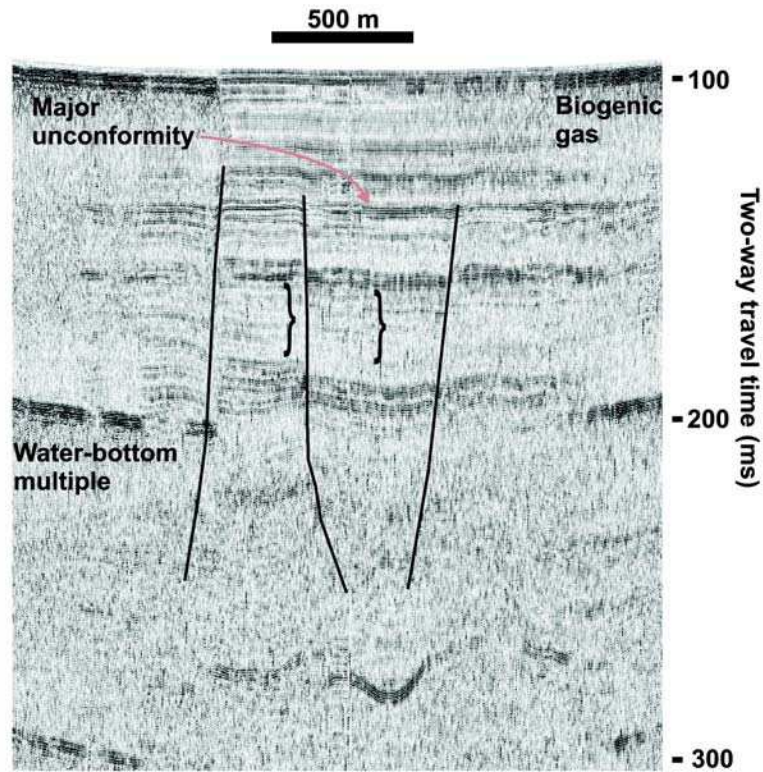


Fig. 7. High-resolution boomer profile extending across the lake from northwest to southeast. Interpreted faults show offset at high levels within the sedimentary section, with observable offsets as shallow as ~40 ms (30 m) sub-bottom. This suggests activity on these structures within the past 150 kyr. Brackets indicate zone of thickening on hanging wall block, indicating syndepositional faulting. Note deformation (gentle folding) of deeper primary reflections, likely due to differential compaction of the impact breccia.

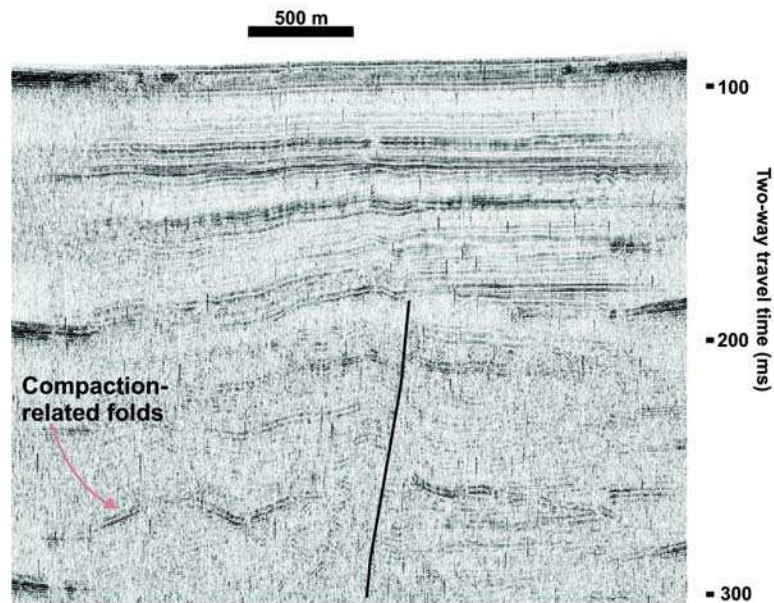


Fig. 8. High-resolution boomer profile extending across the lake from north to south, and illustrating further gentle folding of initially flat-lying lacustrine sediments. Deeper, high-amplitude reflections are likely high-density lacustrine sediment horizons, possibly produced by lake desiccation, and are not the top of the central uplift.

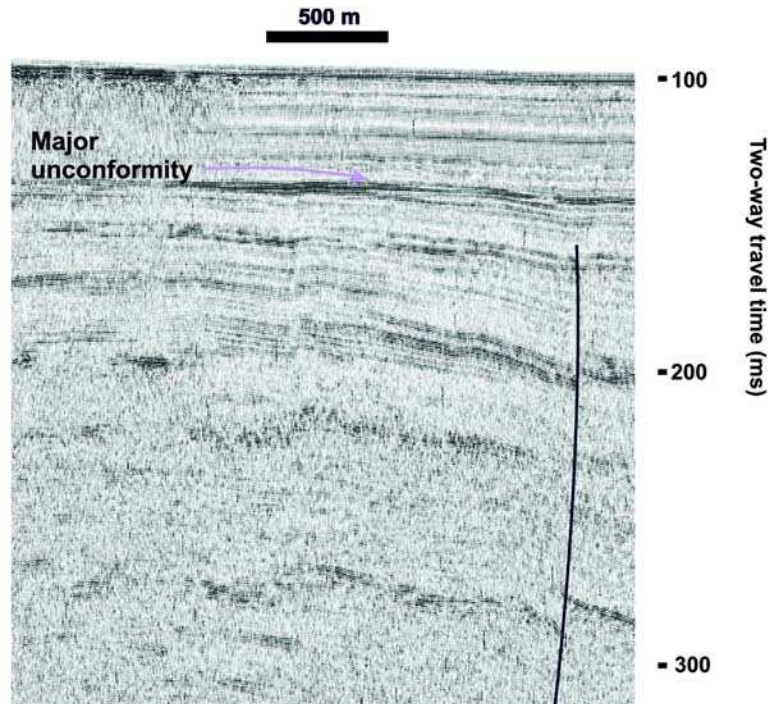


Fig. 9. High-resolution boomer profile extending across the lake from north to south, revealing another mid-sedimentary section normal fault. Note high-amplitude reflection marked as major unconformity, produced during a lake desiccation event within the past 100 kyr. There are several high-frequency reflections that are truncated beneath this high-amplitude event, signifying localized erosion.

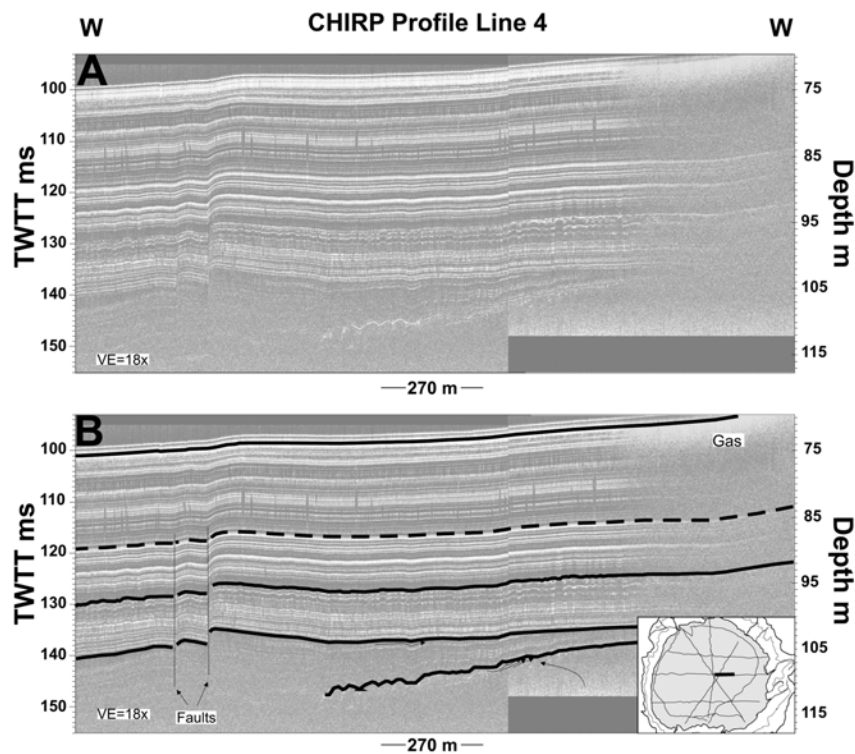


Fig. 10. High-resolution W-E CHIRP profile, modified from Brooks et al. (2005). a) Raw profile. b) Interpreted section. Only part of profile is shown here. Note faults that appear to extend to within 20 m of the water-sediment interface in this profile. Interpreted surfaces are lake lowstand horizons interpreted by Brooks et al. (2005), thought to have developed over the past ~100 kyr.

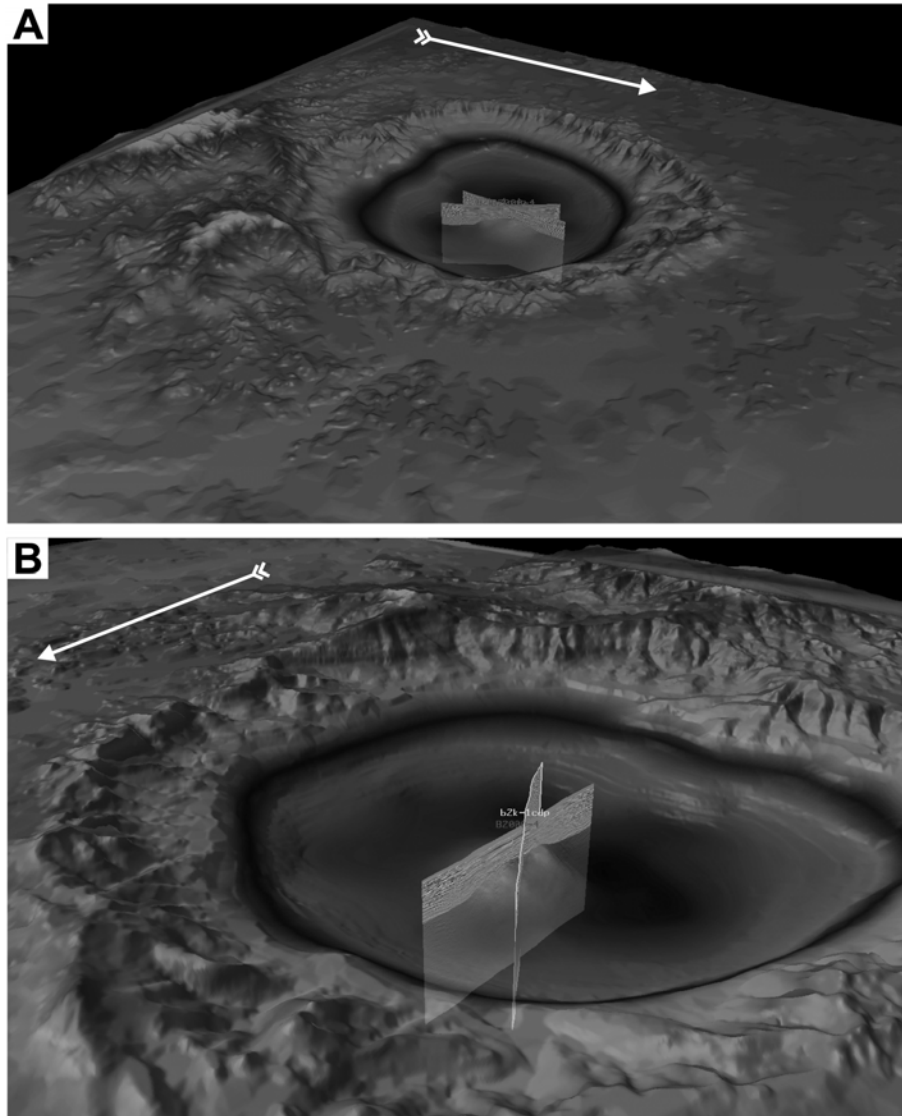


Fig. 11. Two perspectives of a digital elevation model of the Bosumtwi crater from combined regional topography, and the interpreted impactite subsurface horizon. Two multichannel seismic reflection profiles are embedded within each image. a) View from the northeast. b) View from the northwest. High-relief region to the southeast outside the crater rim is the Obuom Range. Subtle outer ring feature is evident in panel A, well outside the main crater rim.

structures. In the case of the Bosumtwi structure the Ivory Coast strewn field is well constrained, and extends to the south and west of the structure. There are no documented asymmetries in deformation structures around the crater rim at Bosumtwi, and thus more detailed studies in this area may be warranted in order to better assess the trajectory of the Bosumtwi impactor.

A comparison of the geometry of the Bosumtwi impact structure with predictions of the uplift structure derived from classic scaling laws (Croft 1985; Cintala and Grieve 1994) has been described in Scholz et al. (2002). An analysis of this sort of the Bosumtwi structure is important because this structure may represent a transition form between simple craters (<4 km) and large complex craters (e.g., Grieve et al.

1995; Melosh 1989). Because central uplift structures develop from the uplift of deeper target rocks within a few seconds of impact, their generation is attributed to elastic rebound of the target rocks and additionally, the gravitational collapse of transient crater (Melosh 1989). The density of the impactor, target rock rheology, and the angle of impact also constrain the final structure geometry (e.g., Schultz and D'Hondt 1996).

The measured data reveal a crater with a slightly higher aspect ratio than predicted from the empirical equations (e.g., Pike 1985), which may be a result of the formation of the central uplift in a gravity field somewhat larger than that of lunar and Martian craters, which were mainly used in the development of the classical scaling laws.

SUMMARY AND CONCLUSIONS

Eight profiles of marine-type MCS data were acquired in a radial pattern across the lacustrine part of the Bosumtwi impact structure, and these data were augmented by two high-resolution seismic reflection surveys, using 1 kHz “boomer” and CHIRP techniques. A well-defined central uplift is observed near the north-central part of the lake. The central uplift is buried under a section of post-impact lacustrine sediments more than 300 m thick in some localities; this feature has a diameter of 1.9 km and a maximum height of 130 m above the annular moat, with an irregular upper surface, and small graben on the peak of the uplift. A series of normal faults extend as much as 120 m into the sedimentary section above the central uplift, and are observed in the airgun as well as high-resolution seismic reflection data. The normal faults were likely generated by ongoing compaction of the high-porosity materials that comprise the central uplift.

A digital elevation model (DEM) was generated by combining the subsurface interpretations with topography from outside the lake. Measurements derived from the DEM indicate a crater with a slightly higher aspect ratio than predicted from the empirical equations, which may be a consequence of an impact in a gravity field somewhat larger than that of lunar and Martian craters, which were mainly used in the development of the classical scaling laws. Future geophysical investigations of the Bosumtwi crater may benefit from using four-component bottom-cable technology to better image through near-surface gas-charged sediments.

Acknowledgments—We thank the people of Ghana, and especially the residents of Abono and other surrounding lakeshore communities for their assistance in completing this survey work. Many individuals, too numerous to identify individually, contributed extensively to the successful field efforts. This paper benefited from helpful reviews by S. Colman, K. Attoh, and C. Koeberl. Support for the geophysical acquisition was provided by the U.S. National Science Foundation Earth System History program. Seismic processing, interpretation, and visualization software was provided to Syracuse University on a grant from Landmark Graphics Corporation.

Editorial Handling—Dr. Christian Koeberl

REFERENCES

- Attoh K. and Ekwueme B. N. 1997. The West African shield. In *Greenstone belts*, edited by de Wit M. J. and Ashwall L. D. Oxford: Oxford University Press. pp. 517–528.
- Brooks K., Scholz C. A., King J. W., Peck J., Overpeck J. T., Russell J. M., and Amoako P. Y. O. 2005. Late-Quaternary lowstands of Lake Bosumtwi, Ghana: Evidence from high-resolution seismic reflection and sediment-core data. *Paleogeography, Paleoclimatology, Paleocology* 216:235–249.
- Castanõ J. R., Clement J. H., Kuykendall M. D., and Sharpton V. L. 1997. Source-rock potential of impact craters. In *Ames structure in northwest Oklahoma and similar features: Origin and petroleum production*, edited by Johnson K. S. and Campbell J. A. Oklahoma Geological Survey Circular #C100. Norman, Oklahoma: University of Oklahoma. pp. 100–103.
- Cintala M. J. and Grieve R. A. F. 1994. The effects of differential scaling of impact melt and crater dimensions on lunar and terrestrial craters: Some brief examples. In *Large meteorite impacts and planetary evolution*, edited by Dressier B. O., Grieve R. A. F., and Sharpton V. L. GSA Special Paper #293. Boulder, Colorado: Geological Society of America. pp. 51–59.
- Croft S. K. 1985. The scaling of complex craters. Proceedings, 15th Lunar and Planetary Science Conference. pp. C828–C842.
- Grieve R. A. F. 1997. Terrestrial impact structures: Basic characteristics and economic significance, with emphasis on hydrocarbon production. In *Ames structure in northwest Oklahoma and similar features: Origin and petroleum production*, edited by Johnson K. S. and Campbell J. A. Oklahoma Geological Survey Circular #C100. Norman, Oklahoma: University of Oklahoma. pp. 3–16.
- Grieve R. A. F., Rupert J., Smith J., and Therriault A. 1995. The record of terrestrial impact cratering. *GSA Today* 5:189, 194–196.
- Jones W. B., Bacon M., and Hastings D. A. 1981. The Lake Bosumtwi impact crater, Ghana. *Geological Society of America Bulletin* 92:1342–1349.
- Karp T., Milkereit B., Janle P., Danuor S. K., Pohl I., Berckhemer H., and Scholz C. A. 2000. Geophysical signature of the Bosumtwi impact crater (abstract). *Eos* 81:F799.
- Kirschner C. E., Grantz A., and Mullen M. W. 1991. Impact origin of the Avak structure, Arctic Alaska, and genesis of the Barrow gas fields. *American Association of Petroleum Geologists Bulletin* 76:651–679.
- Koeberl C. and Shirey S. B. 1993. Detection of a meteoritic component in Ivory Coast tektites with rhenium-osmium isotopes. *Science* 261:595–598.
- Koeberl C., Bottomley R., Glass B. P., and Storzer D. 1997. Geochemistry and age of Ivory Coast tektites and microtektites. *Geochimica et Cosmochimica Acta* 61:1745–1772.
- Leube A., Hirdes W., Mauer R., and Kesse G. O. 1990. The early Birimian Supergroup of Ghana and some aspects of its associated gold mineralization. *Precambrian Research* 46:139–165.
- MacLaren M. 1931. Lake Bosumtwi, Ashanti. *Geographical Journal* 78:270–276.
- Melosh H. J. 1989. *Impact cratering: A geologic process*. Oxford: Oxford University Press. 245 p.
- Peck J. A., Heil C., King J. W., Scholz C. A., Shanahan T. M., Overpeck J. T., Fox P. A., Amoako P. Y., Forman S. L., Koeberl C., and Milkereit B. 2005. The Lake Bosumtwi Drilling Project: A 1 Ma West African paleoclimate record (abstract #PP13C-02). American Geophysical Union Fall Meeting. CD-ROM.
- Pike R. J. 1985. Some morphologic systematics of complex impact structures. *Meteoritics* 20:49–68.
- Plado J., Pesonen L. J., Koeberl C., and Elo S. 2000. The Bosumtwi meteorite impact structure, Ghana: A magnetic model. *Meteoritics & Planetary Science* 35:723–732.
- Poag C. W., Hutchinson D. R., Colman S. M., and Lee M. W. 1999. Seismic expression of the Chesapeake Bay impact crater. In *Impact cratering and planetary evolution II*, edited by Sharpton V. L. and Dressler V. O. GSA Special Paper #339. Boulder, Colorado: Geological Society of America. pp. 149–164.
- Scholz C. A., Karp T., Brooks K. M., Milkereit B., Amoako P. Y. O., and Arko J. A. 2002. Pronounced central uplift identified in the

- Bosumtwi impact structure, Ghana, using multichannel seismic reflection data. *Geology* 30:939–942.
- Schultz P. H. and D'Hondt S. 1996. Cretaceous-Tertiary (Chicxulub) impact angle and its consequences. *Geology* 24:963–967.
- Smit A. F. J. 1964. Origin of Lake Bosumtwi (Ghana). *Nature* 203: 179–180.
- Talbot M. R. and Delibrias G. 1980. A new late-Pleistocene-Holocene water-level curve for Lake Bosumtwi, Ghana. *Earth and Planetary Science Letters* 47:336–344.
- Vail P. R. 1987. Seismic stratigraphy interpretation using sequence stratigraphy. In *Atlas of seismic stratigraphy*, edited by Bally A. W. AAPG Studies in Geology #27. Tulsa, Oklahoma: American Association of Petroleum Geologists. pp. 1–10.
- Wagner R., Reimold W. U., and Brandt D. 2002. Bosumtwi impact crater, Ghana: A remote sensing investigation. In *Meteorite impacts in Precambrian shields*, edited by Plado J. and Pesonen L. J. Berlin: Springer-Verlag. pp. 189–210.
-